

LATTICE VIBRATION SPECTRA OF A_4BX_6 GROUP CRYSTALS

A. I. Kashuba^{1,2}, M. V. Solovyov¹, T. S. Maliy¹, I. A. Franiv³,
O. O. Gomonnai⁴, O. V. Bovgyra¹, O. V. Futey², A. V. Franiv¹, V. B. Stakhura¹

¹Physics Faculty, Ivan Franko National University of Lviv
8, Kyrylo and Mefodiy St., Lviv, UA-79005, Ukraine

²Electronics and Computer Technology Faculty, Ivan Franko National University of Lviv
107, Tarnavski St., Lviv, UA-79017, Ukraine

³Lviv Polytechnic National University, 12, Bandera St., Lviv, UA-79013, Ukraine

⁴Physics Faculty, Uzhgorod National University, 54, Voloshina St., Uzhgorod, UA-88000, Ukraine
e-mail: MVSolovyov@ukr.net

(Received January, 25, 2018)

We report on an X-ray diffraction study of A_4BX_6 (Tl_4HgI_6 and Tl_4CdI_6) group crystals. Structure data and atomic coordinates have been obtained by Rietveld method. The compounds of Tl_4HgI_6 and Tl_4CdI_6 are isomorphous with each other and crystallize in a tetragonal lattice with the space group of $P4/mnc$. The results of the infrared and Raman spectra of Tl_4HgI_6 and Tl_4CdI_6 crystals are present. On the basis of a factor group analysis and phonon frequencies calculated for Tl_4HgI_6 and Tl_4CdI_6 , the relations between the vibrational spectra and the crystal structures have been determined. Moreover, the distribution of vibrations for symmetry classes of single crystals and the selection rules for vibrations in the infrared absorption and Raman spectra are obtained. Phonon modes frequencies and their origin determination are based on Raman scattering data.

Key words: Raman spectra, infrared absorption, crystals, lattice, group theory analysis.

DOI: <https://doi.org/10.30970/jps.22.2701>

PACS number(s): 78.30.-j

I. INTRODUCTION

Now reports are being published in the periodical literature which deal with the possibility of obtaining one class of A_4BX_6 (Tl_4HgI_6 and Tl_4CdI_6) group crystals and studying their optical, mechanical and spectral characteristics [1–10]. Obviously, obtaining new single crystals puts forward the priority task of investigating their basic physical and chemical characteristics: X-ray structural parameters (for Tl_4CdI_6 present in [11]), the temperature dependence of the linear expansion coefficient in the region of phase transitions [11,12], determination of the band gap [13], establishment of the basic optical characteristics [1,2,8,10–14], investigation of luminescence spectra [2,14] and their interpretation.

The prospects of the compounds under study stem from their practical application as working elements of temperature sensors and detectors of ionizing radiation [7]. That is, these are the materials with controlled physical parameters which are promising for optoelectronics and nonlinear optics.

At the same time, there is no information about Tl_4HgI_6 and Tl_4CdI_6 infrared (IR) absorption and Raman spectra, and our current knowledge of vibrational phonon properties is rather limited [8]. Understanding the specifics of phonon and Raman spectrum of those structures can help in the development of Tl_4HgI_6 and Tl_4CdI_6 based optical and electronic devices.

Thus, the aim of this study was to provide further insight into the structure of A_4BX_6 group crystals by means of Raman spectroscopy. In this paper, we present the results of the studies of X-ray diffraction, IR and Raman spectra of Tl_4HgI_6 and Tl_4CdI_6 crystals.

II. SPECIMENS AND THE METHOD OF THE EXPERIMENT

In order to synthesise thallium cadmium (mercury) iodide, we used commercially produced salts of the relevant metal halides. The initial components were taken according to equimolar ratios. The preliminary purification of the salts was by repeated using reiterated recrystallisation from the melt in quartz ampoules, and a vacuum sublimation. Tl_4HgI_6 and Tl_4CdI_6 single crystals were grown with a standard Bridgman–Stockburger technique. The detailed description of the crystals growth setup can be found in Refs. [11,12]. Samples of the grown crystals are presented in Fig. 1.



Fig. 1. Typical photo image of studied Tl_4HgI_6 crystal.

The structure data, atomic coordinates and interatomic distances calculation are based on experimental X-ray

diffraction data. The X-ray powder diffraction (XRPD) data for the X-ray phase analysis and crystal structure refinement were collected in the transmission mode on a STOE STADI P diffractometer [15] at the room temperature of 295 K. The detailed XRPD setup description can be found in Refs. [11,16].

IR absorption spectra of Tl_4HgI_6 and Tl_4CdI_6 were obtained on an automatic dual-beam spectrometer UR-20 in the absorption interval of 200 cm^{-1} to 5000 cm^{-1} [17]. The samples under study were small-thickness ($\sim 2.5\text{ mm}$) plane-parallel plates and perfect optical surfaces. All measurements were made in unpolarized light.

Raman studies were performed using DFS-52 double monochromator. A photomultiplier FEU-136 operating in the photon counting regime was used as a photodetector. The measurements were conducted in normal conditions at room temperature. The solid state and He-Ne laser was used as an excitation source.

III. RESULTS AND DISCUSSION

A. Crystal structure

According to the X-ray phase analysis, the synthesized crystals are practically single-phase samples of the Tl_4HgI_6 and Tl_4CdI_6 compound, space group $P4/mnc$ (point group $4/mmm$), stable at normal conditions. Figure 2 presents a typical XRPD pattern for a Tl_4HgI_6 sample as an example. The unit cell of both crystals consists of two formula units $Z = 2$ and consists of 22 atoms respectively. The calculated cell parameters are shown in Table 1 and values of the atomic coordinates are presented in Table 2. Lattice parameters difference ($b - a$) is zero within the experimental accuracy, and thus the studied crystals must belong to the middle symmetry. The structure is illustrated in Figure 3.

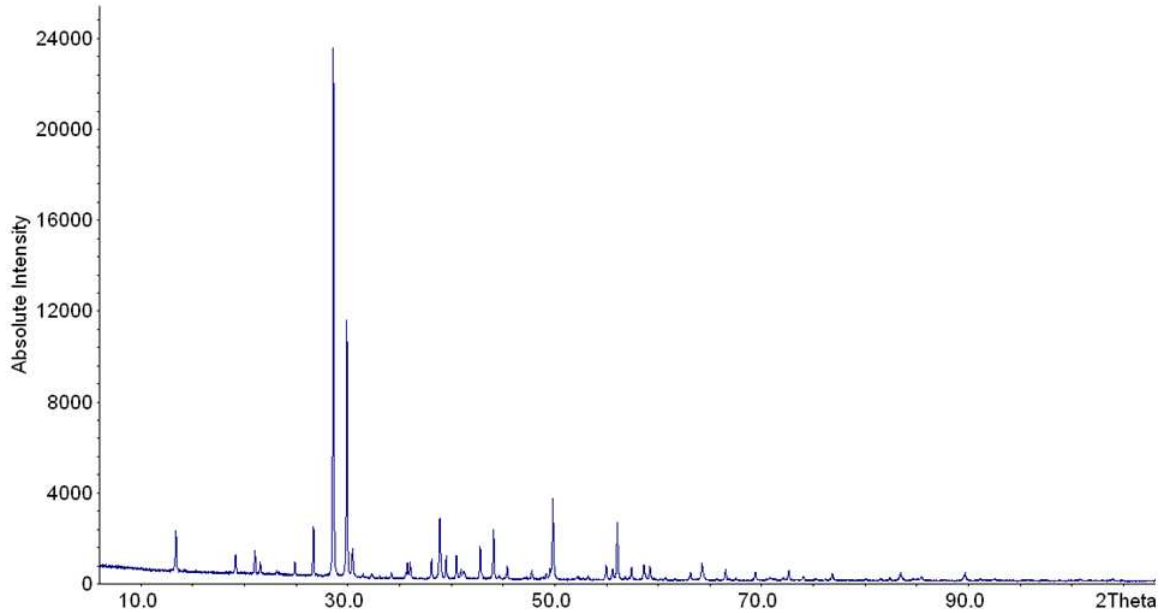


Fig. 2. Room-temperature diffractogram of Tl_4HgI_6 crystals.

Crystal	Tl_4HgI_6	Tl_4CdI_6
$a, \text{Å}$	9.446	9.231
$b, \text{Å}$	9.446	9.231
$b - a, \text{Å}$	0	0
$c, \text{Å}$	9.260	9.592
Z	2	2
$V, \text{Å}^3$	826.24	817.35
$\alpha, ^\circ$	90	90
$\beta, ^\circ$	90	90

Table 1. Some crystallographic parameters of the crystals Tl_4HgI_6 and Tl_4CdI_6 [17].

Atom	Wyck. position	Site	x/a	y/b	z/c
Tl_4HgI_6					
Tl	8g	..2	0.3537	0.8529	0.25
Hg	2a	4/m..	0	0	0
I1	8h	m..	0.3315	0.1449	0
I2	4e	4..	0	0	0.2841
Tl_4CdI_6					
Tl	8g	..2	0.1465	0.6465	0.25
Cd	2a	4/m..	0	0	0
I1	8h	m..	0.1406	0.3161	0
I2	4e	4..	0	0	0.2888

Table 2. Atomic coordinates of the crystals Tl_4HgI_6 and Tl_4CdI_6 .

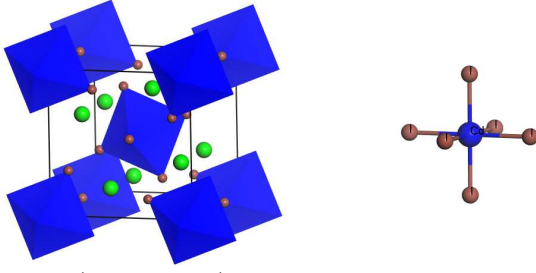


Fig. 3. (Color online). The crystal structure and coordination of Cd ions in Tl_4CdI_6 : Tl – green, I – red, Cd – blue balls.

B. Theoretical calculation of phonon modes

On the basis of the factor group analysis and phonon frequencies calculated for Tl_4HgI_6 and Tl_4CdI_6 , the relations between the vibrational spectra and the crystal structures have been determined [18–20]. The equation that defines the operations group D_{4h}^6 :

$$D_{4h}^6 = D_4^2 + D_4^2 \cdot t(0, 0, \tau) \cdot h_{25} \quad (1)$$

where $h_{25} = (-x, -y, -z)$ is inversion.

The group theory analysis results in the following classification of the A_4BX_6 (Tl_4HgI_6 and Tl_4CdI_6) lattice vibration modes in the Γ point of the Brillouin zone:

$$\Gamma_\nu = 4A_{1g} + 4A_{1u} + 5A_{2g} + 5A_{2u} + 4B_{1g} + 3B_{1u} + 3B_{2g} + 2B_{2u} + 7E_g + 11E_u. \quad (2)$$

The A_{2u} and E_u modes are acoustic (Γ_α). According to (2), 46 optical modes (Γ_o) respond to normal vibrations, namely, to the fully symmetrical, external translation, and are close to libration ones. An expansion of the Γ_α and Γ_o representation gives:

$$\Gamma_\alpha = 4A_{2u} + E_u, \quad (3)$$

$$\Gamma_\nu = 4A_{1g} + 4A_{1u} + 5A_{2g} + 4A_{2u} + 4B_{1g} + 3B_{1u} + 3B_{2g} + 2B_{2u} + 7E_g + 10E_u. \quad (4)$$

By using selection rules, we got active modes in IR (active modes is u) and Raman spectra (g). The Raman active A_{1g} modes correspond to nonzero diagonal elements of the polarizability tensor and are of the highest intensity.

C. IR absorption spectra

The recorded experimental IR spectra for the Tl_4HgI_6 and Tl_4CdI_6 at room temperature in the region 200–5000 cm^{-1} are shown in Fig. 4. These crystals exhibited an overall transmission between 18% and more than 70% for Tl_4HgI_6 (18% to 50% for Tl_4CdI_6) in the IR spectral range.

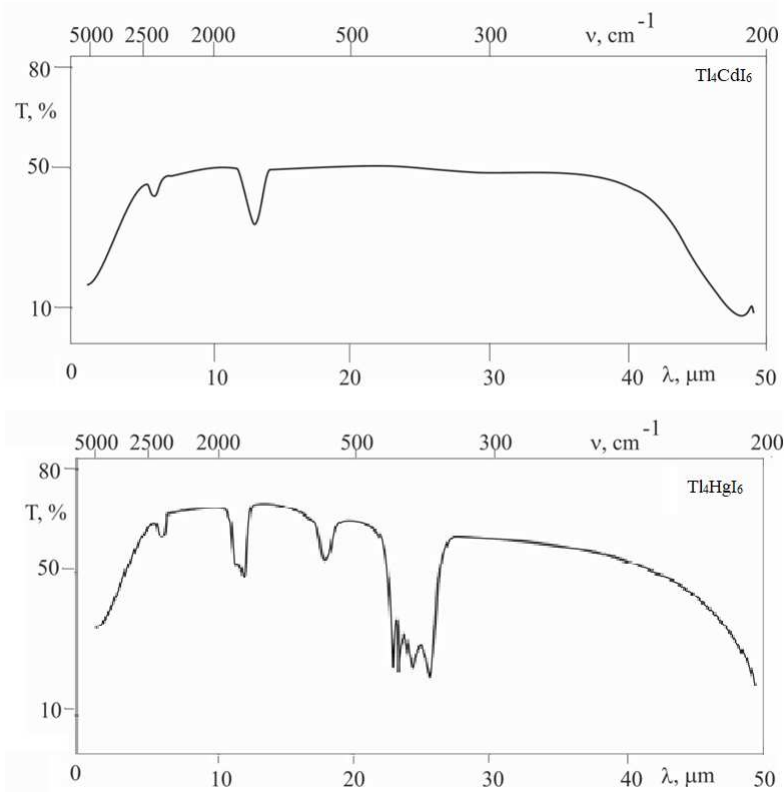


Fig. 4. IR spectra of Tl_4HgI_6 and Tl_4CdI_6 .

The inspection of the spectra shows two absorption bands at 5.1–6.1 μm and 11.9–13.9 μm for Tl_4CdI_6 . These bands are local, and the second one's (11.9–13.9 μm) relative intensity is three times higher than the first one's (5.1–6.1 μm). The IR spectra of a Tl_4HgI_6 crystal can be divided into four main groups localized in spectral regions: 5.4–6.2 μm , 10.9–13.0 μm , 17.9–19.7 μm and 23.2–27.9 μm . The first band, observed near 5–6 μm , and the second one, near 11–13 μm , are very similar for both samples. The third and the fourth bands are unique and they have no analogues in the Tl_4CdI_6 . The optical absorption is significant for the fourth band ($T \sim 18\%$, $\lambda \sim 23.2\text{--}27.9 \mu\text{m}$). At higher frequencies, a gradually increasing absorption caused by electronic transitions is observed.

D. Raman spectra

Figure 5 shows the Raman spectra of Tl_4HgI_6 and Tl_4CdI_6 obtained at room temperature. The most intense spectral feature in both crystals is the high-frequency band at 104.8 cm^{-1} for Tl_4CdI_6 (135.2 cm^{-1} for Tl_4HgI_6). The mode involving the symmetric modulation of CdI_6 (HgI_6) octahedron possesses the highest intensity in the spectra due to its high polarizability.

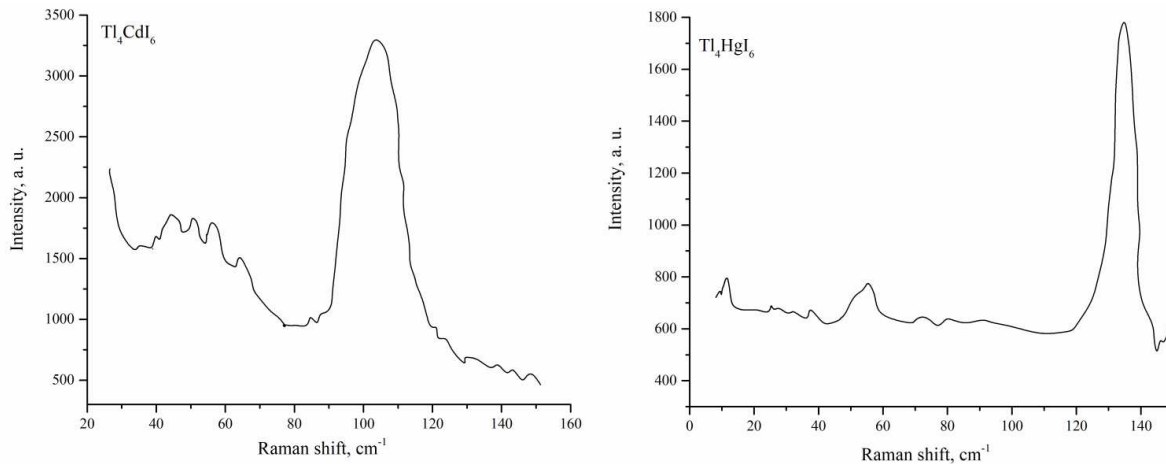


Fig. 5. Raman spectra of Tl_4HgI_6 and Tl_4CdI_6 .

IV. CONCLUSIONS

On the basis of the XRPD patterns analysis of the Tl_4HgI_6 and Tl_4CdI_6 crystals, it was established that the compound crystallizes in an orthorhombic structure with $P4/mnc$ space group. The cell parameters and atomic coordinates in Tl_4HgI_6 and Tl_4CdI_6 were calculated from the XRPD analysis. On the basis of the factor group analysis, it was found out that the phonon spectra of Tl_4HgI_6 and Tl_4CdI_6 crystals contain 48 vibrating modes of 10 types (A_{1g} , A_{2g} , B_{1g} , B_{2g} , A_{1u} , A_{2u} , B_{1u} , B_{2u} , E_u , E_g), which include 46 optical and 2 acoustic modes in the Γ point of the Brillouin zone.

This peak is attributed to the symmetric vibrations of the nearly perfect CdI_6 (HgI_6) octahedron [2]. Concerning the molecular vibration modes of an isolated CdI_6 (HgI_6), there exist $\text{Cd}(\text{Hg})\text{--I}$ stretching and bending modes.

The Tl atoms are distributed to several sites in the Tl_4HgI_6 and Tl_4CdI_6 unit cell, therefore, it is difficult to estimate the number of the whole Raman active phonon modes in the compound. The Raman spectra, due to the vibration modes of Tl–I lattices in Tl_4HgI_6 and Tl_4CdI_6 , are expected to be observed in the low frequency region. But the TII second phase impurity is too low in concentration to be detected by Raman spectroscopy.

In order to make a possible attribution of the modes, we turn to the analysis of the results of *ab initio* calculations [18,21–23]. The active modes in the Tl_4HgI_6 and Tl_4CdI_6 were calculated in the generalized gradient approximation (GGA) with the Perdew–Burke–Ernzerhof (PBE) functional [24].

We suppose that the bands at 104.8, 63.5, 44.8 cm^{-1} for Tl_4CdI_6 (135.2 cm^{-1} for Tl_4HgI_6) frequencies correspond to the A_{1g} vibrating mode, which is allowed and the most intensive one in the spectra, and the peaks at 55.4, 51.7 and 26.5 cm^{-1} for Tl_4CdI_6 (54.9 and 14.2 cm^{-1} for Tl_4HgI_6) frequencies correspond to B_{2g} and E_g modes.

The IR spectra of the Tl_4HgI_6 crystal can be divided into four main groups localized in spectral regions: 5.4–6.2 μm , 10.9–13.0 μm , 17.9–19.7 μm and 23.2–27.9 μm (5.1–6.1 μm and 11.9–13.9 μm for Tl_4CdI_6).

The experimental Raman spectra curve exhibits one intensive peak at 104.8 cm^{-1} for Tl_4CdI_6 (135.2 cm^{-1} for Tl_4HgI_6). This peak is attributed to symmetric vibrations of the nearly perfect CdI_6 (HgI_6) octahedron. The bands of the highest intensity for the Tl_4HgI_6 and Tl_4CdI_6 crystals correspond to the A_{1g} vibrating mode, which is allowed and most intensive one in the spectra. We assume that the impurity of the TII structural phase may be present in our crystal. But, it is too low to be detected using traditional Raman spectroscopy.

- [1] M. Piasecki, M. G. Brik, I. V. Kityk, *Mat. Chem. Phys.* **163**, 562 (2015).
- [2] S. Wang *et al.*, *Cryst. Growth Des.* **15**, 2401 (2014).
- [3] H. Nagase, Y. Furukawa, D. Nakamura, *Bull. Chem. Soc. Jpn* **63**, 3329 (1990).
- [4] S. M. Nair, A. I. Yahya, A. A. Rafiuddin, *Solid State Ion.* **86-88**, 137 (1996).
- [5] M. S. Nawaz, A. A. Rafiuddin, *Ionics* **13**, 35 (2007).
- [6] D. S. Kalyagin, Y. E. Ermolenko, Y. G. Vlasov, *Russi. J. Appl. Chem.* **81**, 2172 (2008).
- [7] D. Kahler *et al.*, *Nucl. Inst. Meth. Phys. Research A* **652**, 1, 183 (2011).
- [8] D. V. Badikov *et al.*, *Inorg. Mater.* **40**, 314 (2004).
- [9] R. L. Ammlung *et al.*, *J. Solid State Chem.* **21**, 185 (1977).
- [10] K. I. Avdienko *et al.*, *Opt. Mater.* **2-3**, 569 (2003).
- [11] A. V. Franiv *et al.*, *Ukr. J. Phys. Opt.* **14**, 6 (2013).
- [12] M. Piasecki *et al.*, *J. Mater. Sci.: Mater. Electron.* **24**, 1187 (2013).
- [13] V. Franiv *et al.*, *Opt. Appl.* **44**, 317 (2014).
- [14] M. Solovyov *et al.*, in *IEEE International Young Scientists Forum on Applied Physics and Engineering YSF-2017* (2017), p. 195.
- [15] Stoe WinXPOW. Version 3.03 (Darmstadt, Stoe and Cie GmbH, 2010).
- [16] O. V. Parasyuk *et al.*, *Mat. Chem. Phys.* **187**, 156 (2017).
- [17] V. A. Franiv, Ph.D. Thesis (Lviv University, 2015).
- [18] I. V. Semkiv *et al.*, *J. Nano- Electron. Phys.* **8**, 30051 (2016).
- [19] A. I. Kashuba, S. V. Apunevych, *J. Nano- Electron. Phys.* **8**, 1, 10101 (2016).
- [20] H. Poulet, J. P. Mathieu, *Vibration Spectra and Symmetry of Systals* (Gordon and Breach, New York, 1976).
- [21] A. I. Kashuba *et al.*, *Funct. Mater.* **23**, 026 (2017).
- [22] A. V. Franiv *et al.*, *Ukr. J. Phys.* **62**, 679 (2017).
- [23] A. I. Kashuba *et al.*, *Ukr. J. Phys. Opt.* **19**, 1 (2018).
- [24] J. P. Perdew, K. Burke, M. Ernzerhof, *Phys. Rev. Lett.* **77**, 3865 (1996).

ДИНАМІКА ҐРАТКИ КРИСТАЛІВ ГРУПИ A_4BX_6

A. I. Кашуба^{1,2}, М. В. Соловійов¹, Т. С. Малий¹, І. А. Франів³, О. О. Гомоннай⁴, О. В. Бовгира¹,
О. В. Футей², А. В. Франів¹, В. Б. Стахура¹

¹Фізичний факультет, Львівський національний університет імені Івана Франка,
вул. Кирила і Мефодія, 8, Львів, 79005, Україна

²Факультет електроніки та комп'ютерних технологій,
Львівський національний університет імені Івана Франка,
вул. Тарнавського, 107, Львів, 79017, Україна

³Національний університет "Львівська політехніка", вул. С. Бандери, 12, Львів, 79013, Україна

⁴Фізичний факультет Ужгородський національний університет,
вул. Волошина, 54, Ужгород, 88000, Україна

Повідомлено про структурні дослідження кристалів групи A_4BX_6 (Tl_4HgI_6 і Tl_4CdI_6). Параметри кристалічної ґратки та положення атомів в елементарній комірці визначено методом Рітвельда. Установлено, що Tl_4HgI_6 і Tl_4CdI_6 є ізоморфними та кристалізуються в тетрагональній кристалічній ґратці просторової групи $P4/mnc$. Подано результати експериментальних досліджень спектрів комбінаційного розсіювання та інфрачервоних спектрів кристалів Tl_4HgI_6 і Tl_4CdI_6 . На основі теоретико-групового аналізу зроблено симетрійну класифікацію фононних мод. Зокрема встановлено розподіл коливань досліджуваного монокристала за класами симетрії, а також визначено правила відбору коливань для інфрачервоних спектрів та спектрів комбінаційного розсіювання. За спектрами комбінаційного розсіювання ідентифіковано положення смуг та зроблено припущення про їх походження.